Synthesis, TEM characterization and thermal behaviour of LiNiSiO pyroxene

Tribaudino, M, Bromiley, G, Ohashi, H & Nestola, F 2009, 'Synthesis, TEM characterization and thermal behaviour of LiNiSiO pyroxene' *Physics and chemistry of minerals*, vol 36, no. 9, pp. 527-536.

DOI: 10.1007/s00269-009-0298-y

Synthesis, TEM characterization and thermal behaviour of $LiNiSi_2O_6$ pyroxene

Authors:

Mario Tribaudino
Dipartimento di Scienze della Terra, Università di Parma, Viale Usberti 157/A, I-43100, Parma, Italy
Tel.: +39 0521 905340
E-mail address: mario.tribaudino@unipr.it

Geoffrey Bromiley
1. Department of Earth Sciences, University of Cambridge Downing Street, Cambridge C2B 3EQ, U.K
2. Bayerisches Geoinstitut, Universität Bayreuth, Germany
E-mail address: gbro04@esc.cam.ac.uk now of University of Edinburgh.

Haruo Ohashi
Hashi Institute for Silicate Science, Nishinakanobu 1-9-25, Shinagawa, Tokyo 142-0054, Japan
E-mail address: haruohashi@hotmail.com

Fabrizio Nestola
Dipartimento di Geoscienze, Università di Padova, Corso Garibaldi 37, I-35137, Padova, Italy
Tel.: +39 049 8272009
E-mail address: fabrizio.nestola@unipd.it

Corresponding author: Mario Tribaudino
Dipartimento di Scienze della Terra, Università di Parma, Viale Usberti 157/A, I-43100, Parma (Italy)
Tel.: +39 0521 905343
E-mail address: mario.tribaudino@unipr.it

Synthesis, TEM characterization and thermal behaviour of $LiNiSi_2O_6$ pyroxene

[1]Dipartimento di Scienze della Terra, Università di Parma, Via Usberti 157/A, I-43100, Parma (Italy)
[2]Dipartimento di Geoscienze, Università di Padova, Corso Garibaldi 37, I-35137, Padova (Italy)

Abstract

A pyroxene with composition $LiNiSi_2O_6$ was synthesized at T = 1473 K and P = 2.0 GPa; the cell parameters at 298 K are a = 9.4169(6) Å, b = 8.4465(7) Å, c = 5.2464(3) Å, β = 110.534(6)°, V = 390.78(3) $Å^3$. TEM examination of the $LiNiSi_2O_6$ pyroxene showed the presence of $h+k$ odd reflections indicative of a $P2_1/c$ space group and of antiphase domains obtained by dark field imaging of the critical reflections.

A HT in situ investigation was performed by examining TEM selected area diffraction patterns collected at high temperature and synchrotron radiation powder diffraction. In HTTEM the $LiNiSi_2O_6$ was examined together with $LiCrSi_2O_6$ pyroxene. In $LiCrSi_2O_6$ the $h+k$ odd critical reflections disappear at about 340 K; they are sharp up to the transition temperature and do not change their shape through the transition. In $LiNiSi_2O_6$ the critical reflections are present up to sample deterioration at 650 K.

A high temperature synchrotron radiation investigation was performed on $LiNiSi_2O_6$ between 298 and 773 K. The analysis of critical reflections and of changes in cell parameters shows that the space group is $P2_1/c$ up to the highest temperature. The comparative analysis of the thermal and spontaneous strain contributions in $P2_1/c$ and $C2/c$ pyroxenes indicates that the high temperature strain in $P2_1/c$ $LiNiSi_2O_6$ is very similar to that due to thermal strain only in spodumene and that a spontaneous strain contribution related to pre-transition features is not apparent in $LiNiSi_2O_6$.

A different mechanism of the high temperature phase transition in $LiNiSi_2O_6$ with respect to other pyroxenes is suggested, possibly in relation with the presence of Jahn-Teller distortion of the M1 polyhedron centered by low spin Ni^{3+}.

Keywords: pyroxene, high temperature TEM observation, high temperature powder diffraction, Ni, phase transition.

Introduction

The structural and crystal chemical behaviour of pyroxenes provides a simple model to test relations between structure and composition within a silicate family. Among pyroxenes those with the M2 site occupied by Li are a peculiar group. The general formula of Li-pyroxenes is $LiM^{3+}Si_2O_6$; in nature only the end member with Al as M^{3+} cation is found, named spodumene, but end members with M^{3+} = Al, Fe, Cr, Ni^{3+},V, Ga, In, Sc and intermediate compositions have been synthesized and studied (Brown 1971, Grotenpass et al 1983, Sato et al 1994, Sato et al 1995, Redhammer et al 2001, Knopin et al 2003, Redhammer et al 2004a). The wide compositional variability on the M^{3+} site provides a model to test the composition-structure relations in pyroxenes. A comparison of the crystal chemical trends in Li pyroxenes with respect to Na-pyroxenes and to pyroxenes with divalent cations at the M2 site is of interest in assessing models on the effect of crystal chemistry on structural arrangement, and on phase transitions (Ohashi and Sato 2003, Redhammer and Roth 2004a). Li pyroxenes are also of interest for the displacive $P2_1/c$ – $C2/c$ phase transition with temperature, found in end members with M^{3+} = Fe, Cr, V, Ga, Sc, at a critical temperature slightly above or below room temperature (Behruzi et al. 1984, Sato et al. 1994, Redhammer et al. 2001), and carefully studied by Redhammer and Roth (2004b). This transition is results from differences in configuration of the tetrahedral chains in $P2_1/c$ and

*C*2/*c* pyroxenes: in $P2_1/c$ pyroxenes there are two different tetrahedral chains, with opposite rotation sense, that become symmetry equivalent in the high temperature *C*2/*c* structure. The *C*2/*c* chain is as a rule more elongated than each of the $P2_1/c$ chains, being almost straight in several Li pyroxenes (M^{3+} = Fe, Cr, V, Ga). The transition is structurally the same as observed in Ca-poor clinopyroxenes of the quadrilateral at high temperature (Arlt et al 2000, Tribaudino et al 2002), but in Li-pyroxenes the transition can be studied at relatively low temperature, between 100 and 350K. Moreover, the compositional variability in Li pyroxenes provides a test for the effect of cation substitution on the phase transition. A negative correlation between cation radius in the M2 site and the critical temperature has been found (Arlt et al 2000, Redhammer and Roth 2004b), but the differences in critical temperature in Li pyroxenes indicate that it is also affected by the M1 cation. A negative correlation between the critical temperature and the radius of the M1 cation is found in Li pyroxenes with V, Ga, Fe and Cr in the M1 site, and for those between the Sc and In end members, but not for those intermediate between $LiScSi_2O_6$ and $LiFe^{3+}Si_2O_6$, which do not show significant changes in the critical temperature. Moreover, applying the Cr to V trend to the Al end member, i.e. to spodumene, implies that it should show the $P2_1/c$ symmetry up to about 700K, while actually it retains the *C*2/*c* structure down to 54K (Tribaudino et al 2003a).

In testing models on composition and phase transition temperature in Li-pyroxenes a limitation exists due to a gap in cation radius between Al and Cr (0.535 vs 0.615Å, Shannon 1976). This gap can be filled by analysis of $LiNiSi_2O_6$ pyroxene: Ni^{3+} in octahedral coordination has a cation radius intermediate with that of Cr^{3+} and Al (0.56 in low spin state for Ni^{3+} vs 0.615 and 0.535 for Cr^{3+} and Al).

At present, however, very few data exist on the end member with $M^{3+} = Ni^{3+}$. This pyroxene was first synthetized by Ohashi and Osawa (1988) at high pressure; the authors gave cell parameters, but no further crystallographic information. Following the trend

outlined by V to Cr pyroxenes, and for a low spin configuration, the Ni end member should undergo the $P2_1/c$ -$C2/c$ symmetry at about 500 K. However, the lack of transition in spodumene suggests caution even in assuming that $LiNiSi_2O_6$ has a $P2_1/c$ symmetry. Moreover the evolution of cell parameters with temperature is not known for $LiNiSi_2O_6$.

This paper reports the *in situ* high temperature cell evolution up to 773 K of a synthetic $LiNiSi_2O_6$ pyroxene and the high temperature TEM investigation of the evolution of critical reflections in $LiNiSi_2O_6$ and $LiCrSi_2O_6$, studied for comparison. The studied samples were previously characterized by TEM observation.

The aim of this work is to report the results of a new synthesis of $LiNiSi_2O_6$, to clarify the room temperature symmetry of $LiNiSi_2O_6$, and to outline the evolution with temperature. Although the phase transition was not achieved for $LiNiSi_2O_6$ the observed evolution of cell parameters with temperature, very similar to that observed in spodumene, poses interesting constrains in the cell *vs* T evolution in Li-pyroxenes.

Experimental

Synthesis

The $LiNiSi_2O_6$ pyroxene was synthesised using a stoichiometric starting mix of Li_2SiO_3 + NiO + SiO_2 (finely ground under ethanol for 2 hours in an agate ball mill). The starting mix was loaded into a 5 mm outer diameter, 4.6 mm inner diameter 10 mm long Pt10-%Rh capsule with 15% H_2O_2 solution, and welded shut. H_2O_2 solution was used to speed reaction, to aid crystal growth, and to react with and oxidise NiO. The capsule was placed in a 0.5 inch pyrex-talc piston-cylinder assembly containing an internal, tapered, graphite furnace. Experiments were performed using an end-loaded piston-cylinder device at the Bayerisches Geoinstitut, Universität Bayreuth. The experiment was initially pressurised to P = 2.0 GPa, and then heated at a rate of 100 degrees per minute to 1473 K, whilst

maintaining pressure. Pressure and temperature were then maintained automatically for 2 hours. After this, the temperature was slowly ramped down to 600 degrees over 3 days, at constant pressure. When this final temperature was reached, power to the heating circuit was switched off to quench the experiment. The recovered capsule was pierced, weighed, heated in an oven and reweighed to check that water was still present after the experiment. This demonstrated that no water/solution was lost. The sample studied in this work was successfully obtained at the end of a series of previously unsuccessful experiments that used varied oxygen fugacity and starting mixtures. The following starting mixes: $NiO+SiO_2+Li_2CO_3$, $NiO+SiO_2+Li_2CO_3$ with 10% H_2O added, $NiO+SiO_2+Li_2O_2$, and $Li_2Si_2O_5+NiO+SiO_2$ were used. The main difficulty in successfully synthesising $LiNiSi_2O_6$ pyroxene appears to be maintaining the high oxidation state of Ni: over time, there is a decrease in fO_2 in the piston-cylinder runs due to the inherent reducing conditions present (due to use of talc and graphite components). Unsuccessful synthesis resulted in $LiNi_2O_4$ + Ni_2SiO_4 assemblages, plus a variable amount of NiO and negligible amount of $LiNiSi_2O_6$ pyroxene.

The $LiCrSi_2O_6$ pyroxene used for TEM high temperature study was from the batch synthesized by Ohashi and Sato (2003).

Sample characterization

X-ray powder diffraction and spin state

The sample was preliminarily investigated by X-ray powder diffraction. Successful synthesis yielded an assemblage of $LiNiSi_2O_6$ pyroxene and $LiNi_2O_4$ spinel. The cell parameters for $LiNiSi_2O_6$ pyroxene are in excellent agreement with those of Ohashi and Osawa (1988), obtained in a synthesis in which Li-pyroxene was the only phase obtained from stoichiometric starting materials. SEM-EDS analysis was performed on a few grains of

pyroxene, and showed no deviation from the expected stoichiometry of Ni and Si. The pyroxene is present as thin elongated crystals less than 20 μm in length.

In the synthesis by Ohashi and Osawa (1988) the $LiNiSi_2O_6$ pyroxene was very sensitive to pressure release, breaking down at room pressure after few days or weeks. The crystals had the to be kept under pressure in a diamond anvil cell. In the present synthesis, possibly as the crystals are clamed(???) in a spinel matrix such problem was not found.

Preliminary magnetic study shows that there is no magnetic transition over the temperature range 350K to 2K and that the octahedral Ni^{3+} has the low spin state (Isobe, 2006; private communication). That is, the Ni^{3+} bearing clinopyroxene is an S=1/2 spin compound and does not show the spin dimerization. To note, in previous papers (Ohashi and Osawa 1988; 2003) the ionic radius high spin cell for the octahedral Ni^{3+} in the high spin configuration (0.60Å) instead of that in low spin (0.56Å) was used to discuss cell parameters - cation radius trends in $LiM^{3+}Si_2O_6$ pyroxenes.

TEM observations

The $LiNiSi_2O_6$ and $LiCrSi_2O_6$ pyroxenes were characterized by transmission electron microscope (TEM) analysis, using a CM12 side entry electron microscope operating at 120 kV. Mounts were prepared by crushing a few grains of the run products in an agate mortar and subsequent deposition on a holey carbon film.

At room temperature the selected area diffraction patterns (SAED) for both $LiNiSi_2O_6$ and $LiCrSi_2O_6$ pyroxenes showed the presence of $h+k$ odd critical reflections, with reflections stronger in $LiNiSi_2O_6$. These reflections are indicative of the P lattice of the $P2_1/c$ structure; in $LiNiSi_2O_6$ they are slightly elongated, and show a diffuse halo (Fig. 1b), whereas in $LiCrSi_2O_6$ the same reflections are sharp, although weaker. Dark field imaging on the critical reflections revealed faint antiphase domains in $LiNiSi_2O_6$, about 20 nm in size (Fig.

1c). The same domains could not be imaged in the grains of $LiCrSi_2O_6$. They may have been overlooked, due to the very low intensity of the critical $h+k$ odd reflections, but the sharpness of these reflections indicates that the domains in $LiCrSi_2O_6$ are rather large, possibly more than the examined grains (sized 1-2 μm). Some grains were twinned with (100) as composition plane (??). Previous studies of the small amount of sample synthesised by Ohashi and Osawa (1988) also showed a *P* lattice. It is assumed that, by similarity with other pyroxenes, the space group in $LiNiSi_2O_6$ is $P2_1/c$.

High temperature *in situ* investigation

The possible presence of a phase transition was sought by TEM and X-ray synchrotron radiation powder diffraction *in situ* high temperature investigations.

Transmission electron microscopy

In situ *HT* investigation was performed with a Gatan 652 double-tilt heating stage and water cooling (Fig 2). The experimental conditions were the same reported in Tribaudino (2000). For comparison the experiment was also performed on $LiCrSi_2O_6$, whose phase transition is known to occur at 335(2) K (Redhammer and Roth 2004b).

Synchrotron radiation powder diffraction

Synchrotron powder X-ray diffraction (XRPD) data were collected between 298 and 773 K on beamline BM8 GILDA at ESRF (Grenoble, France), using an angle dispersed set-up based on a translating image-plate camera (IP), with fixed wavelength λ = 0.61964 Å (Meneghini et al. 2001). Details on the experimental equipment and the furnace calibration are reported in Tribaudino et al (2003b). The heating rate was 2.4°/min with a run duration of 4h. The 2D images were processed by integrating vertical stripes at constant temperature,

after calibration of the sample to image plate distance and instrumental line shape from the pattern of the reference Si. Isothermal full plate images were also recorded at room temperature.

The full profile diffraction patterns were collected in the 2θ range 9-42°; they were quantitatively analysed within the Rietveld structural refinement approach as implemented in the GSAS (Larson and Von Dreele 2004; Toby 2001) package. A detailed description of the procedures followed in refining cell data can be found in Tribaudino et al. (2003b). The unit-cell parameters at the different temperatures are reported in Table 1, and their comparative changes are shown in Fig. 3.

Results and discussion

High temperature in situ TEM observations in $LiCrSi_2O_6$ and $LiNiSi_2O_6$

The results of comparative high temperature SAED patterns are shown in Fig. 2. The critical $h+k$ odd reflections in $LiCrSi_2O_6$ decrease rapidly in intensity, and disappear at about 330-340 K, in correspondence with the $P2_1/c - C2/c$ transition, leaving only a very diffuse halo. Through the transition the critical reflections do not become elongated, as observed for the $P2_1/c - C2/c$ phase transition in pyroxenes along the join diopside-enstatite (Tribaudino 2000) and for the $P\bar{1}$- $I\bar{1}$ transition in anorthitic feldspars (Van Tendeloo et al. 1989, Tribaudino et al. 2000). The appearance of elongated and diffuse reflections at a given temperature is related to the formation of small elongated dynamic domains close to the transition, in turn pinned by compositional heterogeneities (in pyroxenes, Tribaudino 2000) and/or degree of Al-Si order (in feldspars, Adlhart et al. 1980a,b,; Tribaudino et al. 2000). This interpretation is confirmed by the behaviour of stoichiometric $LiCrSi_2O_6$, which is compositionally homogeneous.

In $LiNiSi_2O_6$ the critical reflections do not change their intensity up to the highest temperature reached by the HTTEM investigation, about 650 K. At higher temperatures the examined crystals degrade, losing crystallinity.

Cell parameters, thermal and spontaneous strain

The cell parameters for $LiNiSi_2O_6$ are shown in Table 1 and Fig. 3. The axial thermal expansion in $LiNiSi_2O_6$ shows the usual pattern found in pyroxenes, with $\alpha_b > \alpha_a > \alpha_c$; the values of the thermal expansion coefficients for α_a, α_b and α_c are 5.7(1), 12.0(3) and 3.9(1) $\cdot$ 10^{-6} /K, respectively.

In Fig. 3 the high temperature cell parameters for $LiNiSi_2O_6$ are compared with those of $LiAlSi_2O_6$ and $LiCrSi_2O_6$ pyroxenes. This comparison is significant as the Ni^{3+} low spin ionic radius is 0.56 Å, intermediate between that of octahedral Al (0.53 Å) and Cr^{3+} (0.62 Å, Shannon 1976) Furthermore, the choice of $LiAlSi_2O_6$ and $LiCrSi_2O_6$ pyroxene as reference phases permits comparison between the thermal expansion of $LiNiSi_2O_6$ with that of a pyroxene that does not show the $P2_1/c - C2/c$ phase transition ($LiAlSi_2O_6$), and one that does ($LiCrSi_2O_6$). In $LiCrSi_2O_6$ the cell parameters (mostly a and β, but also b and c) show clear changes at the transition (Fig 3). These changes are not found in spodumene or $LiNiSi_2O_6$, suggesting that the $P2_1/c - C2/c$ phase transition was not achieved in $LiNiSi_2O_6$, at least over the investigated temperature range. This is confirmed by the presence, also at high temperature, of the $h+k$ odd reflections of the $P2_1/c$ space group. These reflections, generally barely detectable in a powder diffraction pattern, are relatively strong in $LiNiSi_2O_6$ pyroxene (Fig. 4), and their intensity does not decrease at sight(??) with temperature.

The above data do not show evidence of an approach to the transition, such as a decrease in the intensity of critical reflections and/or clear changes in the evolution of the cell parameters with temperature. More subtle changes, indicative of the presence of a significant

spontaneous strain from a higher temperature phase transition, could be shown by the analysis of the strain tensor with temperature.

The deformation of the unit cell with temperature is described by a second rank strain tensor, geometrically represented by a strain ellipsoid. The strain tensor can be calculated between any temperature interval from the low and high temperature cell parameters (Ohashi and Burnham 1973). In a structure without a high temperature phase transition, such as in *C*2/*c* spodumene, the measured strain is only due to thermal expansion, whereas a calculation of the strain performed using high and low temperature cell parameters both below the transition, such as $P2_1/c$ $LiCrSi_2O_6$, will show also a significant contribution from the strain arising from the transition, i.e. the spontaneous strain. The spontaneous strain records the deformation inherent to pre-transition structural changes, that are, as a rule, different and often larger than those due to thermal expansion only. The spontaneous strain may even have an effect very far from the transition, as is the case with the *C*2/c- $C\bar{1}$ phase transition in anorthite, that occurs well above the melting point, but still affects the low temperature thermodynamics of anorthite (Carpenter 1992). The strain ellipsoid tensor in a low temperature phase, e.g the one calculated by comparing the cell parameters of the $P2_1/c$ phase at different temperature in $LiCrSi_2O_6$, should show contributions from both thermal and spontaneous strain, and have quite different size and orientation from the one due to pure thermal strain. Therefore the analysis of the strain tensor with temperature may show whether there is a significant spontaneous strain contribution from the transition of the same kind shown by other $LiM^{3+}Si_2O_6$ pyroxenes, even if the transition is not attained. In $LiNiSi_2O_6$, a significant spontaneous strain contribution would suggest that the transition is likely to occur at a higher temperature.

The strain was calculated in $LiNiSi_2O_6$ and in $LiGaSi_2O_6$, $LiCrSi_2O_6$ and $Ca_{0.15}Mg_{1.85}Si_2O_6$ pyroxenes below the transition, the latter being a Li free pyroxene with

different, more kinked, chain arrangement, but showing the $P2_1/c$- $C2/c$ transition at the critical temperature of about 1200 K (Tribaudino et al. 2002). The $P2_1/c$ - $C2/c$ transition in $LiGaSi_2O_6$ and $LiCrSi_2O_6$ is continuous and second order, whereas in $Ca_{0.15}Mg_{1.85}Si_2O_6$ it is first order. Moreover, for the wide stability range of the $P2_1/c$ phase in $Ca_{0.15}Mg_{1.85}Si_2O_6$, the strain can be calculated from cell parameters well below the transition. The strain was also calculated between unit cells(??) at a temperature above the transition, into the $C2/c$ field, in $LiCrSi_2O_6$, $Ca_{0.15}Mg_{1.85}Si_2O_6$ and, for comparison, in spodumene,

As shown in Table 2, the Li bearing $P2_1/c$ pyroxenes display the major expansion along a direction about 150° from the c axis, on (010), and little or no expansion along the b axis. In $LiCrSi_2O_6$ below the transition the deformation pattern is very similar to that of $LiGaSi_2O_6$, but with higher deformation along the major axis. In $Ca_{0.15}Mg_{1.85}Si_2O_6$ the higher deformation on (010) occurs along a direction close to that of $P2_1/c$ $LiCrSi_2O_6$ and $LiGaSi_2O_6$. The expansion along the b axis is instead significant. The orientation of the major deformation is close to that of the spontaneous strain only (155° from the c axis) calculated for $Ca_{0.15}Mg_{1.85}Si_2O_6$ by Tribaudino et al. (2002), in which negligible components along the other directions were found.

Comparing with thermal strain in the $C2/c$ symmetry the strain in the $P2_1/c$ structure is higher, but the difference is mostly due to a higher deformation along the major axis. The orientation of the thermal strain ellipsoid in $C2/c$ is somewhat different than in $P2_1/c$: the highest deformation or that close to highest is found along the b axis, and the major deformation onto the (010) plane occurs in a direction almost normal to that of the major direction in $P2_1/c$ pyroxenes. It appears that the spontaneous strain has an effect higher than the thermal strain. The contribution of the spontaneous strain can be observed even far away from the transition: in $Ca_{0.15}Mg_{1.85}Si_2O_6$ there seems to be no difference between the strain calculated between room T up to 573 and to 1073K: in both cases the strain follows the

pattern for $P2_1/c$ pyroxenes, i.e. the spontaneous strain is significant even far from the transition.

In spite of the fact that $LiNiSi_2O_6$ has a $P2_1/c$ symmetry, the strain with temperature in $LiNiSi_2O_6$ is fully comparable with that arising uniquely from the thermal strain contribution of spodumene: both show a higher expansion along the b axis, and along a direction between 50-60° from the c axis. A similar pattern of deformation was found in $LiCrSi_2O_6$ above the transition, apart for a lower expansion along the b axis. It appears that the observed deformation with temperature in $LiGaSi_2O_6$ and $LiCrSi_2O_6$ in $P2_1/c$ accounts for a significant spontaneous strain, that cannot be observed in $LiNiSi_2O_6$.

The differences in strain are well accounted by the different behaviour with T of cell parameters in $LiNiSi_2O_6$, $LiAlSi_2O_6$ and $LiCrSi_2O_6$ (Fig. 3): the β cell parameter in spodumene and $C2/c$ $LiCrSi_2O_6$ decrease at the same rate as $LiNiSi_2O_6$, whereas in $P2_1/c$ an increase in the β parameter is generally observed, in Li-pyroxenes but also in Ca-Mg-Fe pyroxenes. This could indicate that even if a phase transition is achieved in $LiNiSi_2O_6$, it may occur with a mechanism quite different from that of other pyroxenes.

It could, alternatively, be suggested that the sample was synthetized within the $C2/c$ field based on the observed presence of antiphase domains, formed as an effect of the decreased lattice symmetry between $C2/c$ and $P2_1/c$ during cooling and decompression. It is not clear however whether the high-pressure conditions are needed to stabilize the $C2/c$ phase.

$P2_1/c$ - $C2/c$ phase transition in Li-pyroxenes

The increasing data set on phase transition temperature, or, as here and in spodumene, on the non-occurrence of the phase transition, can be used to verify any trend relating composition and the critical temperature of the phase transition. An increase in the

critical temperature together with a decrease in ionic radius on the M1 site can actually be found in Cr, Fe, V and Ga (Fig. 5). However, according to this trend spodumene should show $P2_1/c$ symmetry up to about 600K and $LiNiSi_2O_6$ should switch to *C2/c* at about 500K. Even the general observation that increasing cation radius in the M1 site decreases the critical temperature is not always observed. It does between In and Sc, but not between Fe and Sc, which show a slight increase in the critical temperature towards the larger ionic sized Sc. Between $LiGaSi_2O_6$ and spodumene the critical temperature actually decreases in spite of the decreased M1 cation radius.

It appears, therefore, that the main influence(?) is the effect of cation substitutions on the rather flexible pyroxene structure, i.e. changes in the structural configuration are driven by the electronic configuration of the M1 cation, rather than by cation radius. In pyroxenes with the M1 site occupied by transition metals with significant crystal field stabilization energy (CFSE Ti^{3+}, Cr^{3+}, V^{3+}, Ni^{3+}) the transition temperature appears to increase with stabilization energy in octahedral coordination (from $1/5\Delta_0$, $4/5\Delta_0$, $6/5\Delta_0$ to $9/5\Delta_0$, between Ti^{3+}, V^{3+}, Cr^{3+} and low spin Ni^{3+}). In $LiTiSi_2O_6$ the transition was not found down to 183K (Kopnin et al. 2003), in $LiVSi_2O_6$ and $LiCrSi_2O_6$ the transition occurs at 203 and 330 K (Redhammer and Roth 2004b), in $LiNiSi_2O_6$ in excess of 773 K. In pyroxenes along the $LiGaSi_2O_6$– $LiAlSi_2O_6$ join no stabilization energy is present, and a different trend of T_c vs composition is observed, i.e. the T_c decreases. This is most significant when comparing spodumene with $LiNiSi_2O_6$ pyroxene, as these have different stability fields but similar cation radius (Fig. 5). However, as shown by the evolution in the transition temperature between pyroxenes with M^{3+} = Fe, Sc and In, with no CFSE, a general model has yet to be proposed.

A point that should be considered in explaining the anomalous behavour of $LiNiSi_2O_6$ pyroxene is that Ni^{3+} in a low spin state has an unpaired e_g electron, promoting, therefore, a highly distorted M1 polyhedral configuration due to Jahn-Teller effect. This

configuration is anomalous with respect to other pyroxenes, and possibly couples with the phase transition spontaneous strain and critical temperature. Further investigation, involving combined quantomechanical modelling and Rietveld analysis of the diffraction pattern at room temperature is in progress.

References

Adlhart W, Frey F, Jagodzinski H (1980a) X-ray and neutron investigations of the $P\bar{1}$-$I\bar{1}$ transition in pure anorthite. Acta Cryst A36:450-460.

Adlhart W, Frey F, Jagodzinski H (1980b) X-ray and neutron investigations of the $P\bar{1}$-$I\bar{1}$ transition in anorthite with low albite content. Acta Cryst A36:461-470.

Arlt T, Kunz M, Stoltz J, Armbruster T, Angel RJ (2000) P-T-X data on $P2_1/c$ clinopyroxenes and their displacive phase transitions. Contrib Mineral Petrol 138:35-45.

Behruzi M, Hahn T, Prewitt CT, Baldwin K (1984) Low and high temperature crystal structures of $LiFeGe_2O_6$, $LiFeSi_2O_6$ and $LiCrSi_2O_6$. Acta Cryst A40 suppl:C-247.

Brown WL (1973) On Li and Na trivalent-metal pyroxenes and crystal field effects. Mineral Mag 38:43-48.

Cameron M, Sueno S, Prewitt CT, Papike JJ (1973) High temperature crystal chemistry of acmite, diopside, hedenbergite, jadeite, spodumene, and ureyite. Am Mineral 58:594-618

Carpenter MA (1992) Equilibrium thermodynamics of Al/Si ordering in anorthite. Phys Chem Minerals 19: 1-24.

Grotenpaß M, Behruzi M, Hahn, T. (1983) Strukturen, Polymorphie un Mischkristallbildung im System $LiScSi_2O_6$-$LiInSi_2O_6$-$LiScGe_2O_6$-$LiInGe_2O_6$. Zeit Kristall 162:90-91.

Kopnin EM, Sato A, Takayama-Muromachi E. (2003) High pressure synthesis and structure refinement of $LiTiSi_2O_6$. J Alloys Compounds 354:L16-L19

Larson AC, Von Dreele RB (1997) GSAS: General Structure Analysis System. Document LAUR 86-748, Los Alamos National Laboratory.

Redhammer GJ, Roth G, Paulus W, André G, Lottermoser W, Amthauer G, Treutmann W, Koppelhuber-Bitschnau B (2001) The crystal and magnetic structure of Li-egirine $LiFe^{3+}Si2O6$: a temperature-dependent study. Phys Chem Minerals 28:337-346.

Meneghini C, Artioli G, Balerna A, Gualtieri AF, Norby P, Mobilio S (2001) A translating imaging Plate System for in-situ experiments at the GILDA Beamline. J Synchr Rad 8: 1162-1166.

Ohashi H, Osawa T (1988), Syntheses of $LiNiSi_2O_6$ and $LiTiSi_2O_6$ spodumenes. J Jpn Assoc Min Petr Econ Geol 83:308-310.

Ohashi H, Osawa T (2003), Syntheses of $NaNiSi_2O_6$ and $NaYSi_2O_6$ clinopyroxenes. In"X-ray study on Si-O bonding", Haruo Ohashi Ed., Maruzen, Tokyo, ISBN 4-89630-094-7 pp 258-264.

Ohashi H, Sato A. (2003) Studies on $P2_1/c$ $LiM^{3+}Si_2O_6$ pyroxenes, In "X-ray study on Si-O bonding", Haruo Ohashi Ed., Maruzen, Tokyo, ISBN 4-89630-094-7 pp 229-243.

Ohashi Y, Burnham CW (1973) Clinopyroxene lattice deformations: the roles of chemical substitution and temperature. Am Mineral 58:843-849

Redhammer G, Roth G (2004) Structural variation and crystal chemistry of $LiMe^{3+}Si_2O_6$ clinopyroxenes Me^{3+} = Al, Ga, Cr, V, Fe, Sc and In. Zeit Kristall 219:278-294.

Redhammer G, Roth G (2004) Structural changes upon the temperature dependent $C2/c \rightarrow P2_1/c$ phase transition in $LiMe^{3+}Si_2O_6$ clinopyroxenes, Me^{3+} = Cr, Ga, Fe, V, Sc and In. Zeit Kristall 219:585-605.

Sato A, Osawa T , Ohashi H (1994) $LiGaSi_2O_6$. Acta Cryst C50:487-488.

Sato A, Osawa T, Ohashi H (1995) Low- temperature form of $LiGaSi_2O_6$. Acta Cryst C51:1959-1960.

Satto C, Millet P, Galy J (1997): Lithium vanadium metasilicate, $LiVSi_2O_6$. Acta Cryst C53:1727-1728.

Shannon RD (1976) Revised effective ionic radii and systematic studies of interatomic distances in halides and chalcogenides. Acta Cryst A32:751-767.

Toby BH (2001) EXPGUI, a graphical user interface for GSAS. J Appl Crystall 34: 210-213.

Tribaudino M (2000) A transmission electron microscope investigation on the *C*2/*c* -*P*2_1/*c* phase transition in clinopyroxenes along the diopside-enstatite ($CaMgSi_2O_6$-$MgSi_2O_6$) join. Am Mineral 85: 707-715.

Tribaudino M, Benna P, Bruno E (2000) TEM observations on the $P\bar{1}$-$I\bar{1}$ phase transition in feldspars along the join $CaAl_2Si_2O_8$- $SrAl_2Si_2O_8$ Am Mineral 85: 963-970.

Tribaudino M, Nestola F, Cámara F, Domeneghetti MC (2002) The high temperature *P*2_1/*c*-*C*2/*c* phase transition in Fe-free pyroxenes: structural and thermodynamic behaviour. Am Mineral 87:648-657

Tribaudino M., Nestola F., Prencipe M., Rundlof H. (2003a) A single-crystal neutron-diffraction investigation of spodumene at 54 K. Can Mineral 41:521-527.

Tribaudino M, Nestola F, Meneghini C, Bromiley GD (2003b) The high temperature *P*2_1/*c*-*C*2/*c* phase transition in Fe-free Ca-rich *P*2_1/*c* clinopyroxenes. Phys Chem Minerals 30:527-535

Van Tendeloo G, Ghose S, Amelinckx, S. (1989) A dynamical model for the $P\bar{1}$-$I\bar{1}$ phase transition in anorthite, $CaAl_2Si_2O_8$ I. Evidence from electron microscopy. Phys Chem Minerals 16:311-319.

Table 1. Variation of unit-cell parameters with temperature for $LiNiSi_2O_6$. The esd is: in a, b and c respectively 0.0006, 0.0007 and 0.003 Å, in β 0.006°, and in volume 0.03 $Å^3$ for all cell parameters. The uncertainty on the temperature is estimated around 1°C.

T (K)	*a* (Å)	*b* (Å)	*c* (Å)	β (°)	*V* ($Å^3$)
298	9.4169	8.4465	5.2464	110.534	390.78
313	9.4174	8.4480	5.2461	110.528	390.87
338	9.4188	8.4495	5.2473	110.522	391.10
365	9.4197	8.4516	5.2475	110.517	391.26
389	9.4206	8.4535	5.2481	110.502	391.47
415	9.4213	8.4563	5.2488	110.504	391.68
441	9.4232	8.4586	5.2492	110.496	391.91
466	9.4246	8.4609	5.2502	110.483	392.17
491	9.4258	8.4631	5.2506	110.471	392.39
517	9.4270	8.4653	5.2507	110.463	392.58
543	9.4288	8.4670	5.2512	110.461	392.77
569	9.4296	8.4703	5.2513	110.447	393.00
594	9.4308	8.4731	5.2516	110.430	393.25
620	9.4323	8.4755	5.2525	110.423	393.51
645	9.4340	8.4794	5.2530	110.420	393.81
671	9.4349	8.4834	5.2534	110.405	394.10
696	9.4374	8.4867	5.2542	110.397	394.44
722	9.4400	8.4890	5.2551	110.386	394.75
747	9.4415	8.4909	5.2562	110.378	395.00
773	9.4412	8.4925	5.25579	110.360	395.08

Table 2. Size and orientation of the unit strain ellipsoid with temperature. The strain was calculated between the cell parameters at the given temperatures. The angle was given with the positive **c** axis measured towards the positive **a** axis. Data sources: 1) Cameron et al (1973); 2) Redhammer and Roth (2004b); 3) Tribaudino et al (2002); 4) this work

		Unit strain (x 10^{-5}/K)			Angle with **c** (°)		
		ε_1	ε_2	ε_3	ε_1	ε_2	ε_3
*C*2/*c*							
1	$LiAlSi_2O_6$ 298-1023 K	1.05(4)	0.84(3)	0.18(3)	90	52(2)	142(2)
2	$LiCrSi_2O_6$ 355-773 K	1.31(2)	1.12(1)	0.42(2)	53(1)	90	143(1)
3	$Di_{15}En_{85}$ 1298-1423 K	1.25(4)	0.82(5)	-0.01(8)	90	116(2)	16(2)
$P2_1/c$							
4	$LiNiSi_2O_6$ 313-773 K	1.15(2)	0.95(3)	0.25(2)	90	62(1)	152(1)
2	$LiCrSi_2O_6$ 298-323 K	5.8(3)	1.0(5)	0(4)	152(3)	62(3)	90
2	$LiGaSi_2O_6$ 100-250 K	2.58(6)	0.92(8)	-0.14(7)	160(1)	70(2)	90
3	$Di_{15}En_{85}$ 298-573 K	1.4(2)	1.3(2)	0.4(2)	141(9)	90	51(9)
3	$Di_{15}En_{85}$ 298-1073 K	1.64(6)	1.37(7)	0.54(8)	146(3)	90	56(3)
$P2_1/c$ - *C*2/*c* spontaneous strain		Unit strain (x 10^{-3}/K)					
3	$Di_{15}En_{85}$ at 298 K	23.6(8)	-1.7(8)	-1.5(8)	155(1)	65(1)	90

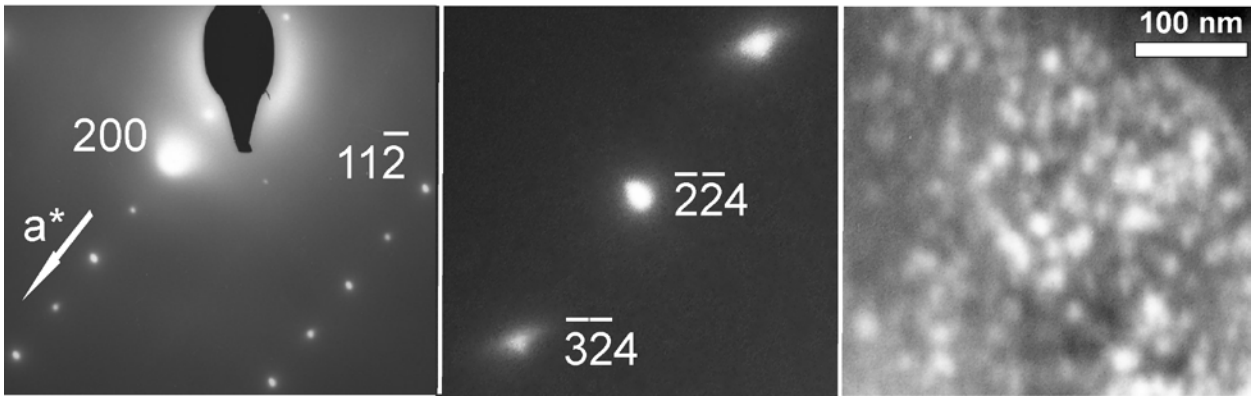

Figure 1. TEM characterization of $LiNiSi_2O_6$. Left: SAED pattern along the $[0\,\bar{2}\,1]$ direction; middle: elongated $h+k$ odd reflections; right: antiphase domains, dark field: **g** = $[21\,\bar{2}]$

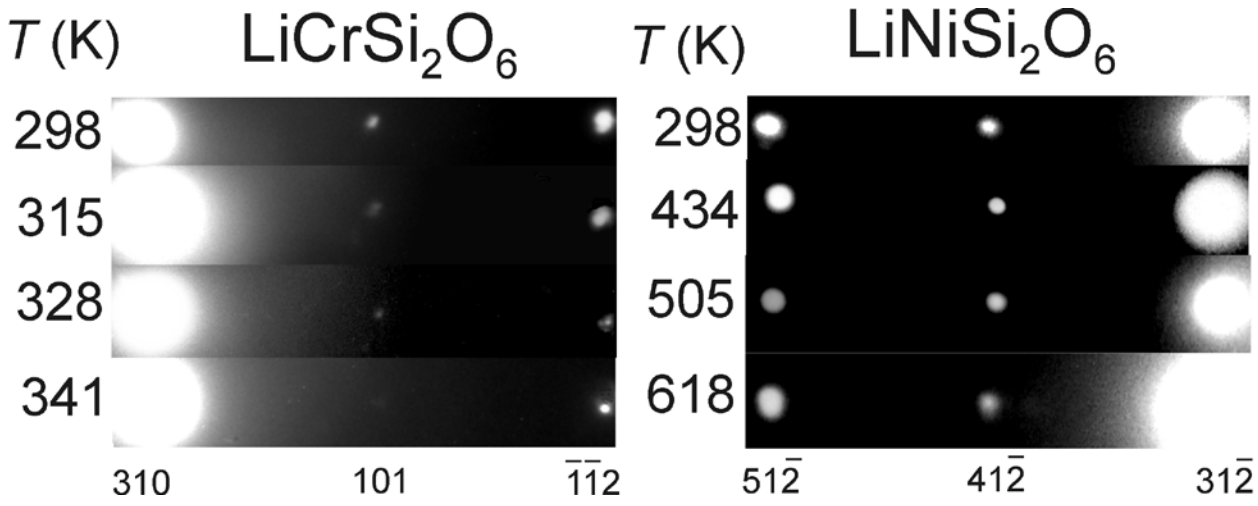

Figure 2. High temperature selected area electron diffraction in $LiCrSi_2O_6$ and $LiNiSi_2O_6$

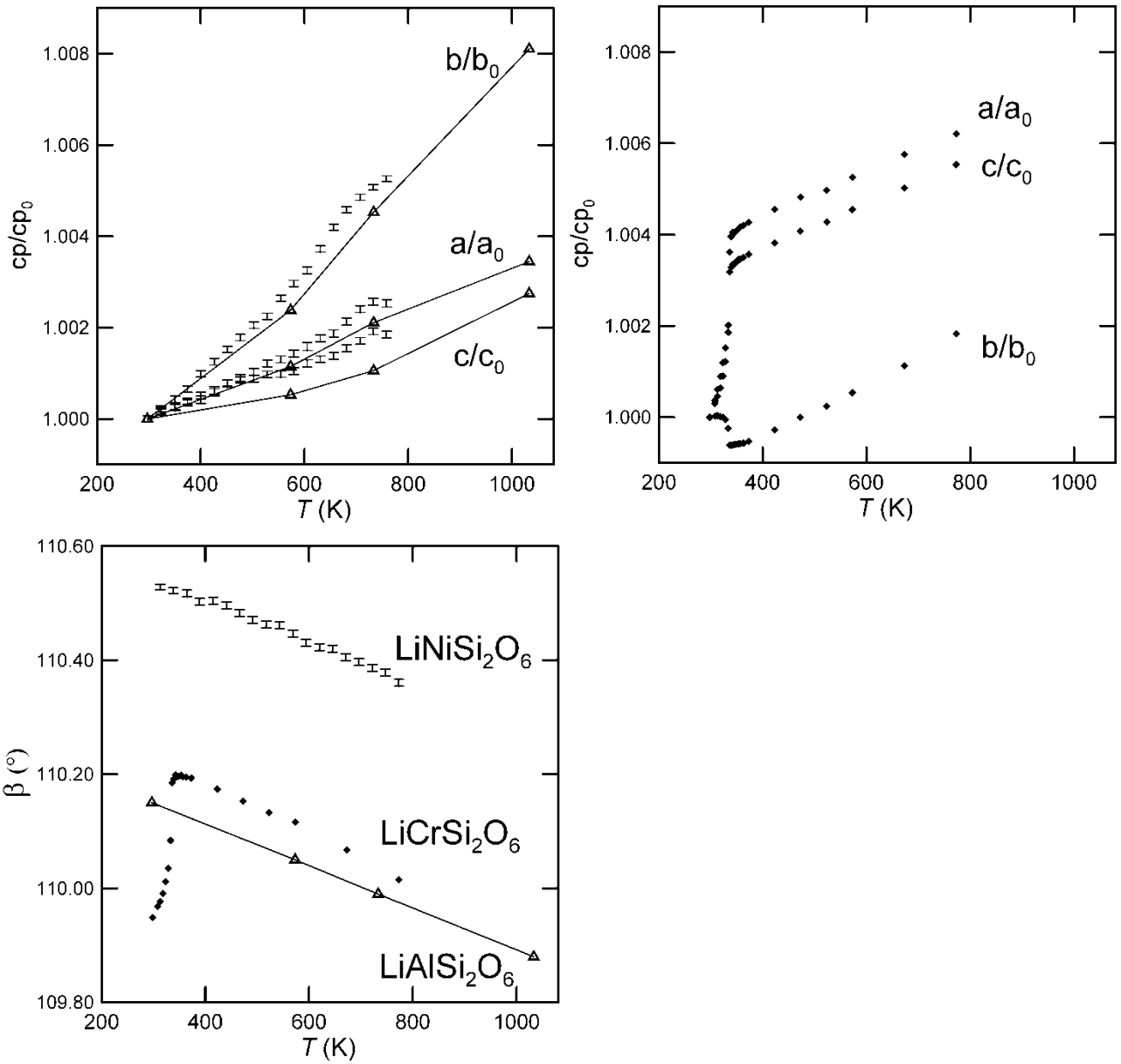

Figure 3. Thermal evolution of cell parameters in $LiNiSi_2O_6$, $LiCrSi_2O_6$ and $LiAlSi_2O_6$. Upper left: normalized cell parameters for spodumene (triangles) and $LiNiSi_2O_6$ (error bars, corresponding to ± 1 esd); upper right: normalized cell parameters for $LiCrSi_2O_6$ (diamonds, note the change at the transition); lower left: β cell parameters.

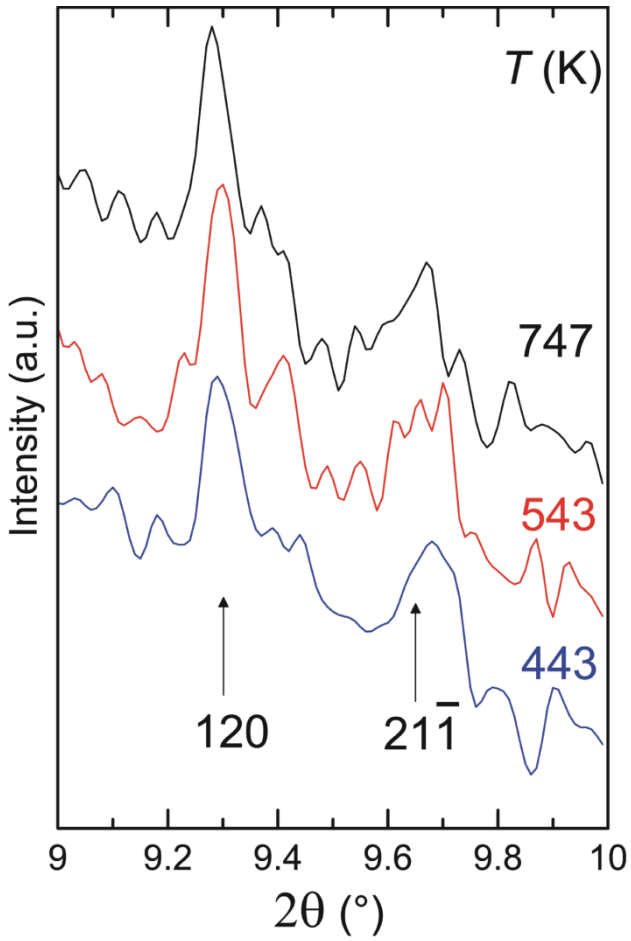

Figure 4. The $h+k$ odd critical reflections 120 and $21\bar{1}$ in power diffraction file at 443, 543 and 747 K. The intensity of the powder diffraction pattern at 773 K is considerably lower and not comparable with the others.

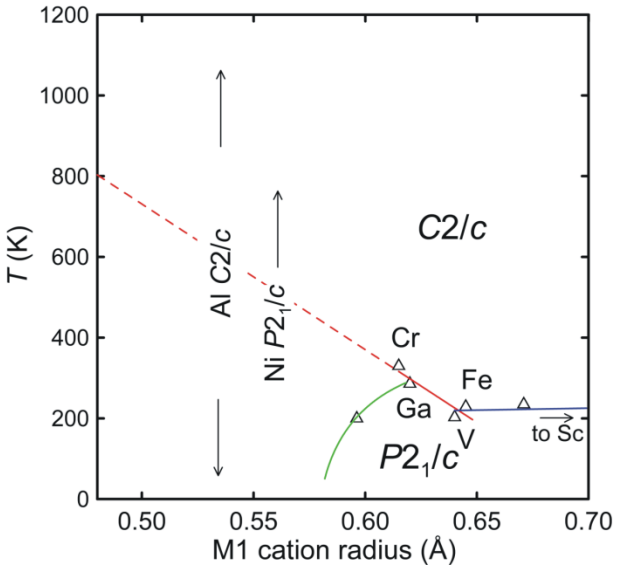

Figure 5. $P2_1/c$-$C2/c$ phase transition boundaries in $LiM^{3+}Si_2O_6$ pyroxenes. Triangles: critical temperatures for $LiM^{3+}Si_2O_6$ pyroxenes with M^{3+} = Fe, Cr, V, Ga, for $LiFe_{0.74}Sc_{0.26}Si_2O_6$ pyroxene (compilation from Redhammer and Roth 2004b) and for $LiGa_{0.72}Al_{0.28}Si_2O_6$ pyroxene (Ohashi and Sato 2003). Blue line: boundary along the join $LiFeSi_2O_6$ and $LiScSi_2O_6$; red line: transition temperature between pyroxenes with M^{3+} = Fe, Cr, V, Ga; red dashed line: extrapolation to lower cation radius of the trend of pyroxenes with M^{3+} = Fe, Cr, V, Ga; green line: boundary along the join $LiGaSi_2O_6$ and $LiAlSi_2O_6$: the trend is based upon the transition temperature in $LiGa_{0.72}Al_{0.28}Si_2O_6$ (about 200 K) and the lack of transition in $LiGa_{0.47}Al_{0.53}Si_2O_6$ down to135 K (Ohashi and Sato 2003).